Available online at www.sciencedirect.com
SCIENCE DIRECT
Journal of Catalysis 235 (2005) 92–102
JOURNAL OF CATALYSIS
www.elsevier.com/locate/jcat

Selective NH_3 oxidation on (110) and (111) iridium surfaces

C.J. Weststrate [a,*], J.W. Bakker [a], E.D.L. Rienks [a], J.R. Martinez [a], C.P. Vinod [a,b], S. Lizzit [c], L. Petaccia [c], A. Baraldi [d,e], B.E. Nieuwenhuys [a,b]

[a] *Leids Instituut voor chemisch onderzoek, Universiteit Leiden, PO Box 9502, Einsteinweg 55, 2333 CC Leiden, The Netherlands*
[b] *Technische Universiteit Eindhoven, Schuit Institute of Catalysis, PO Box 5600 MB, Eindhoven, The Netherlands*
[c] *Sincrotrone Trieste, Strada Statale 14, km 163.5, I-34012 Basovizza, Italy*
[d] *Physics Department and Center of Excellence for Nanostructured Materials, Trieste University, Via Valerio 2, I-34127 Trieste, Italy*
[e] *Laboratorio TASC-INFM, S.S. 14, km 163.5, I-34012 Trieste, Italy*

Received 10 June 2005; revised 22 July 2005; accepted 25 July 2005

Available online 22 August 2005

Abstract

Ammonia oxidation was studied in situ on Ir(110) and Ir(111) under low-pressure ($\sim 10^{-7}$ mbar) conditions. NH_3 does not dissociate on a flat Ir(111) surface, but surface defects and O_{ad} facilitate $NH_{3\,ad}$ decomposition. High-energy resolution fast XPS measurements were used to monitor the surface coverage during reaction on Ir(110), and temperature-programmed reaction measurements were applied to reveal the gas phase reaction products during reaction. The steady-state NH_3 oxidation reaction starts between 350 and 500 K on both surfaces, which also show similar selectivity. Below 600 K, N_2 and H_2O are the principal reaction products. Above 600 K, the selectivity changes to NO and H_2O, with the exact temperature depending on the NH_3:O_2 pressure ratio. The surface population changes from NH_{ad}/N_{ad} to O_{ad} around 500 K, about 200 K lower than the selectivity change from N_2 to NO observed in the gas phase. This behavior can be explained by considering the activation energies for N_2 and NO_{ad} formation. We present a model to explain why Ir is more selective toward N_2 than Pt.

PACS: 82.20.-w; 82.30.-b; 82.45.Jn; 82.65.+r; 82.80.Pv

Keywords: NH_3; Ammonia oxidation; Ir(110); Ir(111); Iridium; X-Ray photoelectron spectroscopy; Selective oxidation; Catalytic surface science

1. Introduction

Since the advent of strict pollution control regulations, clean processes and waste gas stream cleaning have become important issues in the chemical industry. Ammonia is one of the pollutants that must be removed from waste streams. In the environment, NH_3 is converted to nitrite and nitrate. Nitrate contributes to acid rain and can cause unwanted fertilization of surface waters and delicate ecosystems. Ammonia can be removed from a waste stream via oxidation toward N_2 and H_2O, using a heterogeneous catalyst.

Van den Broek, Grondelle, and van Santen [38] have shown that Ir is an active catalyst for the oxidation of NH_3 into N_2 and H_2O. Ir catalysts also show a high selectivity toward N_2 rather than NO_x. Carabineiro and Nieuwenhuys [9,10] investigated the oxidation of NH_3 on Ir(110) and Ir(510) using temperature-programmed desorption (TPD) and temperature-programmed reaction (TPR) between 300 and 800 K. They found that the Ir(110) surface showed selectivity toward N_2, but a small amount of N_2O was also observed. They concluded that Ir(510) is more active and selective (less N_2O) than Ir(110). In contrast to what was reported for Ir(110), Ir(510) and Ir(100) [9,10,12,34,39], NH_3 does not dissociate on Ir(111) [27,32].

In recent work, we discussed some fundamental aspects of adsorption and decomposition of NH_3 on Ir(110), as well as the effect of oxygen on ammonia adsorption and decomposition [39,40]. In these experiments we adsorbed ammonia at a low surface temperature and subsequently heated the

* Corresponding author.
E-mail address: c.westrate@chem.leidenuniv.nl (C.J. Weststrate).

0021-9517/$ – see front matter
doi:10.1016/j.jcat.2005.07.022

surface in vacuum. The results demonstrated that NH_3 decomposition takes place on Ir(110) in both the presence and the absence of O_{ad}. Nitrogen formed via $NH_{3\,ad}$ decomposition desorbs between 500 and 700 K in the absence of O_{ad}. When oxygen is adsorbed before dosing the ammonia, a larger fraction of the $NH_{3\,ad}$ decomposes. O_{ad} especially enhances NH_{ad} dissociation, which would otherwise inhibit $NH_{3\,ad}$ dissociation below the NH_3 desorption temperature (400 K). In the presence of O_{ad} we observed N_2 formation at 350 K, about 200 K lower than in the absence of O_{ad}. This effect of oxygen is assigned to repulsive interactions between N_{ad} and O_{ad} [14,28,40]. NO_{ad}/NO (g) was observed in an experiment where a mixed $O_{ad}/NH_{3\,ad}$ layer was heated in the presence of O_2 ($\sim 1 \times 10^{-7}$ mbar). NO forms when both N_{ad} and O_{ad} are present on the surface and above 450 K.

Several steps in the mechanism responsible for ammonia oxidation on Ir catalysts remain topics of debate. Two mechanisms have been proposed for N_2 formation on Ir and Pt: N_{ad} combination [8,30,39] [Eq. (1)] and $NH_{x\,ad}$ combination [17,19,20] [Eq. (2)]

$$2N_{ad} \rightarrow N_2(g), \tag{1}$$

$$2NH_{x\,ad} \rightarrow N_2(g) + xH_2(g). \tag{2}$$

Similar mechanisms are proposed for NO formation

$$N_{ad} + O_{ad} \rightarrow NO_{ad}, \tag{3}$$

$$NH_{x\,ad} + (x+1)O_{ad} \rightarrow NO_{ad} + xOH_{ad}. \tag{4}$$

Another issue under discussion is the difference in selectivity between Ir and Pt. Bradley, Hopkinson and King [8,26] proposed a reaction model for Pt(100), which is summarized in the following set of equations:

$$2NH_{3\,ad} + 3O_{ad} \rightarrow 2N_{ad} + 3H_2O(g), \tag{5}$$

$$N_{ad} + O_{ad} \rightarrow NO_{ad}, \tag{6}$$

$$NO_{ad} \rightarrow N_{ad} + O_{ad} \quad (>350\ \text{K}), \tag{7}$$

$$2N_{ad} \rightarrow N_2(g), \tag{8}$$

$$NO_{ad} \rightarrow NO(g). \tag{9}$$

Eq. (5) describes O_{ad}-induced $NH_{3\,ad}$ dehydrogenation. N_{ad} formed in this step can desorb as N_2 [Eq. (8)], but the major part reacts with O_{ad} to form NO_{ad} [Eq. (6)]. NO dissociation [Eq. (7)] occurs only above 350 K, and is inhibited when the O_{ad} coverage is larger than 0.2 l. Above 350 K, N_{ad} (formed via NO_{ad} dissociation) desorbs as N_2(g) via Eq. (8). Above 400 K, NO_{ad} desorbs [Eq. (9)], a process favored over dissociation. In this way the selectivity shifts toward NO(g).

Van den Broek et al. [38] extended this model to Ir catalysts and attributed the difference in selectivity between Pt and Ir catalysts to a difference in NO dissociation activity. NO dissociates more easily on Ir than on Pt; in the BHK model this means that the reaction rate of Eq. (7) is larger, and thus N_2 is the principal product.

We report new experimental results for ammonia oxidation on Ir(110), obtained with high-energy resolution fast XPS and TPR. XPS allows us to measure the nature and concentration of different surface species ($NH_{x\,ad}$, O_{ad}, NO_{ad}) in situ during reaction, for different temperatures. This approach, combining information about surface coverage and gas phase products, is a powerful method for investigating the reaction mechanism.

2. Experimental

The TPD and TPR measurements were performed at the Leiden Institute of Chemistry using a vacuum system equipped with a differentially pumped, shielded mass spectrometer, to reduce the contribution from the heating wires and the edges of the crystal. The sample was placed in front of a 2-mm-wide hole, at a distance of ~2 mm. The system is equipped with a sputter gun for sample cleaning, and LEED optics. The base pressure of the system is $<5 \times 10^{-10}$ mbar. A heating rate of 0.5 K/s was used for all TPR experiments. A linear background was subtracted from the TPR results, to correct for the slow increase in the partial pressures, especially for $m/e = 28$ (N_2 and CO) and $m/e = 18$ (H_2O).

For the TPD experiments on Ir(111), a heating rate of 5 K/s was used. In some experiments $^{15}NH_3$ was used to distinguish between N_2 and CO.

High-energy resolution fast XPS measurements [4,6] were performed at the SuperESCA beamline of ELETTRA, the synchrotron radiation facility in Trieste, Italy. The vacuum system, with a base pressure of $\sim 1 \times 10^{-10}$ mbar, is equipped with a double-pass hemispherical electron energy analyzer [7], a sputter gun for sample cleaning, a mass spectrometer, and LEED optics.

Both Ir(110) and Ir(111) surfaces were cleaned with Ar^+ sputtering and annealing cycles (~1200 K), followed by oxygen treatments at 700–1000 K and a final hydrogen treatment to remove oxygen. Residual hydrogen was removed by a flash to 700 K. O1*s* and C1*s* core level regions did not show oxygen or carbon contamination after cleaning on Ir(110). For Ir(111), LEED, AES, and oxygen TPD [24,36] were used to check for surface contaminants. Thermal desorption of an oxygen-covered surface is especially sensitive for surface carbon. Carbon present on the surface forms CO or CO_2 in the presence of O_{ad}, which is then detected during the heating ramp.

N1*s* spectra were measured with a photon energy of 496 eV; O1*s* spectra, with a photon energy of 650 eV. For the temperature-programmed XPS (TP-XPS) [5] measurements, a heating rate of 0.3 K/s was used. The XPS measurements were done only for Ir(110).

The XPS data were evaluated by fitting the spectra with Doniach–Šunjić functions [25], convoluted with a Gaussian function and superimposed on a linear background. Core-level binding energies of the different species were measured with respect to the Fermi level.

According to Ibbotson et al. [36] a surface saturated with O_2 at 200 K results in a coverage of 1 monolayer (ML). This

was used to calibrate the $O1s$ signal. Because we do not have any reference structure for nitrogen we have arbitrarily normalized the sum of all N1s species at 300 K to 1.

The ammonia pressure was 5×10^{-8} mbar during the TP-XPS and 1×10^{-7} mbar during the TPR measurements, respectively, and the O_2 partial pressure was adjusted according to the NH_3:O_2 pressure ratio. A different pressure was used in the TPR experiments to compensate for the shielded MS. Because of the close proximity of the sample surface to the entrance of the differentially pumped MS, the reactant pressure is expected to be slightly lower at the sample surface than in the rest of the vacuum chamber.

3. Results and discussion

3.1. NH_3 decomposition on Ir(111): TPD experiments

TPD and TPR experiments (Fig. 1) were performed to characterize $NH_{3\,ad}$ adsorption and decomposition on Ir(111). Panel (a) shows NH_3 desorption (TPD, 5 K/s) after different exposures to ammonia at 100 K. In these experiments only molecular ammonia desorption was observed, without the formation of N_2(g) and H_2(g). This result confirms the finding of Purtell et al. [32] that $NH_{3\,ad}$ does not decompose on Ir(111).

Panel (b) shows the effect of preadsorbed oxygen on the stability of $NH_{3\,ad}$. The desorption spectra were obtained after the surface was exposed to O_2(10 L at 200 K, saturation) and subsequently exposed to $^{15}NH_3$ (5 L, saturation). Both N_2 and H_2O desorption are observed. In contrast to what was found for the initially clean surface, $NH_{3\,ad}$ dissociated in the presence of O_{ad}, similar to what was observed for several other transition metals, such as Pt, Ni, Cu, and Ag [1,11,16,18,21,22,35,37]. $^{15}N_2$ desorption occurred at around 500 K, a temperature comparable to the N_2 desorption peak measured after NH_3 decomposition from Ir(100), but unlike the N_2 desorption observed from Ir(110) in either the absence (620 K [9,39,40]) or the presence (350 K [40]) of O_{ad}. Water formation occurred between 200 and 400 K, similar to what was observed for Ir(110) [40]. Nitrogen desorption occurred around 500 K, above the H_2O formation temperature. This shows that N_{ad} combination rather than $NH_{3\,ad}$ dehydrogenation is the rate-determining step for N_2 formation. Comparing the $^{15}N_2$ desorption of panel (b) with panel (c), e.g. N_2 formation in the absence of O_{ad} shows that the presence of O_{ad} exerts only a small influence on the N_2 desorption temperature, not as large as that observed for Ir(110) (repulsive interaction [14,28,40]). An explanation for this observation could be that all O_{ad} is consumed during the $NH_{3\,ad}$ dehydrogenation and there is no oxygen left at the temperature where N_{ad} desorption occurs.

The fact that NH_3 dissociates spontaneously on the less densely packed (110) and (100) surface structures Ir(110), but not on Ir(111), suggests that atoms with a low coordination number play an important role in the NH_3 decomposition process. Mortensen et al. [31] reported that the dissociative sticking coefficient of NH_3 on Ru(0001), a close-packed structure, is enhanced when the surface is slightly sputtered. The present study found similar behavior for NH_3 dissociation on Ir(111). Panel (c) shows that $^{15}NH_3$ decomposition occurs as a steady-state reaction (1×10^{-7} mbar $^{15}NH_3$, heating rate 0.5 K/s) after the surface has been sputtered (energy, 2 keV; sample current, ~5 μA, time 0–180 s). The reaction rate reaches a maximum at 580 K and decreases above this temperature. This behavior is very similar to that of steady-state NH_3 decomposition on Ir(110), shown in

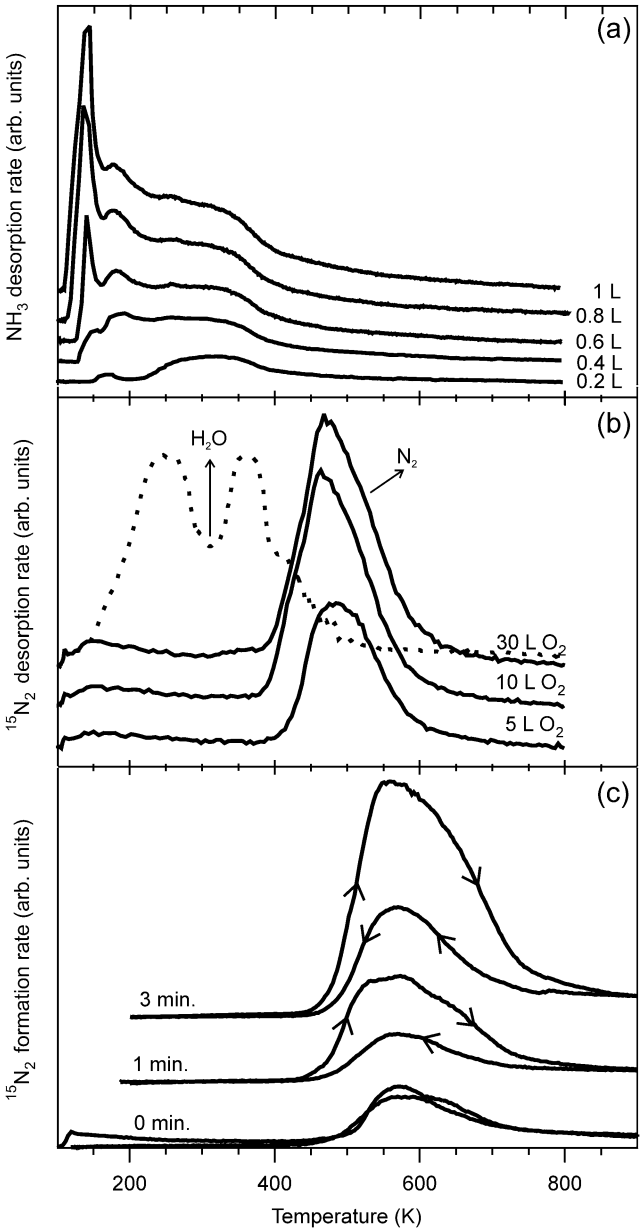

Fig. 1. NH_3 decomposition on Ir(111). (a) Molecular NH_3 desorption after uptake at 100 K (no decomposition observed, heating rate 5 K/s); (b) $^{15}N_2$ desorption after exposure of an O_{ad} covered surface to $^{15}NH_3$ (5 L $^{15}NH_3$, 5 K/s); and (c) steady state $^{15}NH_3$ decomposition on sputtered surfaces ($^{15}NH_3$ pressure 1×10^{-7} mbar, heating rate 0.5 K/s).

Ref. [39], in which a similar maximum was observed at a similar temperature. The fact that the smooth surface (0 min of sputtering) also shows some activity is attributed to defects on the annealed surface. Some authors reported that NH_3 dissociates on Pt surfaces above its desorption temperature [23,30], and this might contribute to the observed activity of the untreated surface as well. For the sputtered surfaces, the heating and cooling branches show significant differences in activity. The maximum temperature reached during the experiments was 1100 K. At this temperature, the surface partially reorders, and thus reactivity is lower in the cooling branch. Our observations support the model proposed by Mortensen et al. [31] in which defects, such as steps and kinks, are responsible for NH_3 dissociation on smooth surfaces like Ru(0001) and Ir(111).

3.2. TPR and XPS measurements during the NH_3/O_2 reaction on Ir(110)

Fig. 2 shows the different N1*s* surface species probed with the high-energy resolution fast XPS measurements during TP-XPS of a coadsorbed layer in NH_3 and O_2 (5×10^{-8} mbar NH_3, 5×10^{-7} mbar O_2). Panel (a) shows two averaged spectra (average of three spectra, at 400 and 580 K) in which the fitting components are shown. Panel (b) shows some of the actual spectra, in which the thermal evolution of the different peaks can be seen. We have previously shown [39,40] that the observed peaks can be assigned to NO_{ad} (400.0 eV), $NH_{3\,ad}$ (399.0 eV), NH_{ad} (397.5 eV) and N_{ad} (396.6 eV) respectively. In one of these publications [39] we suggested that $NH_{2\,ad}$ is a very unstable intermediate that decomposes immediately after formation toward NH_{ad}. Thus, it is not observed in our experiments. In the O1*s* spectra (not shown) obtained during the in situ experiments, O_{ad} (530.5 eV) and NO_{ad} (533.0 eV) were found. Any peaks related to OH or H_2O were not observed above 200 K [40] so the surface concentration of these species was very low under reaction conditions.

Fig. 3 shows the gas phase products (Figs. 3a and c) and the relative concentrations of different surface species measured with XPS (Figs. 3b and d) during subsequent heating-cooling cycles in a reaction mixture of NH_3 and O_2 (1×10^{-7} mbar NH_3, ratio 1:1). Before the surface was exposed to the reaction mixture, it was saturated with O_{ad} (5 L O_2 at 200 K).

The decrease of the O_{ad} signal and the increase of the N_{ad} signal observed on XPS show (Fig. 3b) that the reaction between $NH_{3\,ad}/NH_{ad}$ and O_{ad} occurred between 250–400 K [40]. This resulted in a high N_{ad} concentration at 400 K, with almost all the O_{ad} removed from the surface and formation of both H_2O and $NH_{x\,ad}$ species. The $NH_{x\,ad}$ species block further O_2 adsorption and/or dissociation. Fig. 3a indeed shows H_2O desorption between 200 and 400 K as a result of the reaction of $NH_{3\,ad}/NH_{ad}$ and O_{ad}. No other desorption products were observed below 400 K.

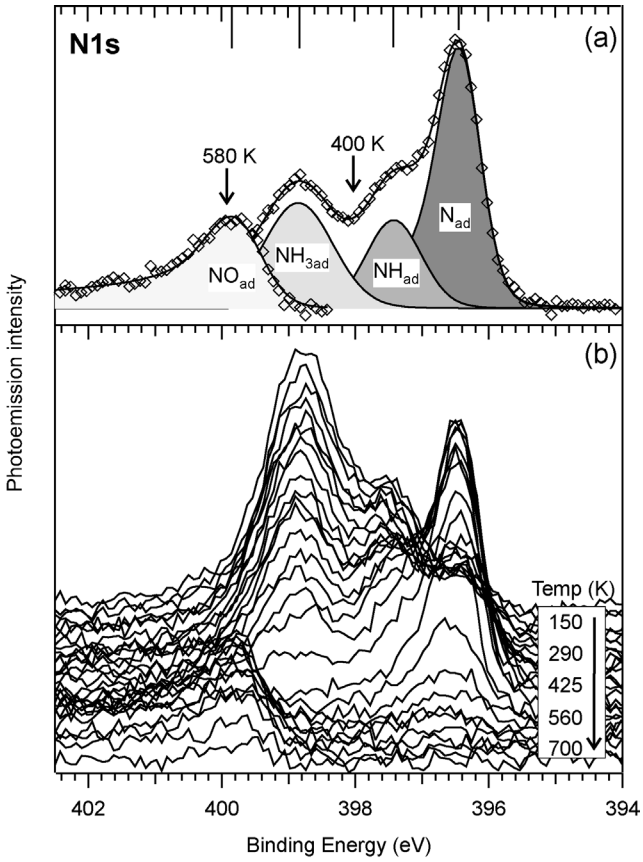

Fig. 2. (a) Two (400 and 580 K, average of three spectra) selected spectra that show the fitting components used to evaluate XP spectra. (b) The actual spectra obtained during a TP-XPS experiment (first heating in a heat–cool–heat sequence, $NH_3/O_2 = 1{:}10$, heating rate 0.3 K/s).

A small N_2 desorption peak was observed between 400 and 500 K and it was assigned to N_2 desorption due to repulsive interaction [13,40] between N_{ad} and O_{ad}. The steady-state reaction started at 450 K, the usual temperature for N_2 desorption in the absence of O_{ad} [39,40]. The XPS results (Fig. 3b) show that the concentration of O_{ad} was very low at this point, resulting in low H_2 production next to H_2O and N_2. The maximum observed in the N_2 formation between 500 and 600 K was related to the desorption of the N_{ad} concentration built up below 450 K. In an experiment with a lower heating rate (0.1 K/s) this peak was absent, indicating that the observed signal was a convolution of the steady-state reaction and a non-steady-state desorption peak.

Above 600 K, the surface composition changed from $NH_{x\,ad}$- to O_{ad}-covered. Intuitively, one would expect that the N-selectivity would also change at the same temperature, that is from N_2 to NO. In earlier work [40] using an experiment in which a mixed $O_{ad}/NH_{3\,ad}$ layer was heated in the presence of O_2, we showed that NO_{ad} formed above 450 K when both N_{ad} and O_{ad} were present on the surface. Under steady-state reaction conditions, we did not observe NO(g) formation below 900 K. We discuss this apparent discrepancy in more detail in Section 3.5.

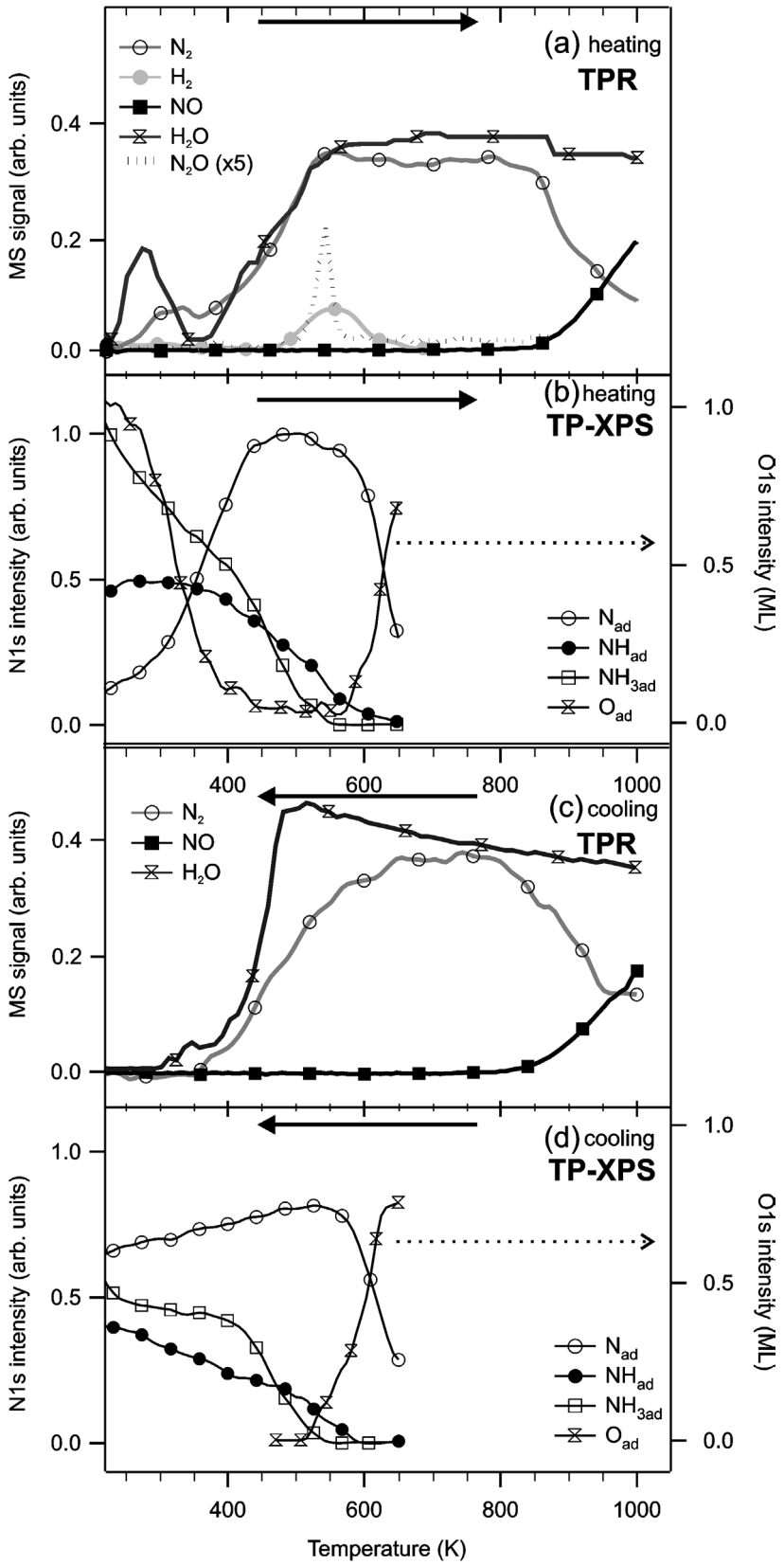

Fig. 3. In situ measurements during the NH_3/O_2 reaction with a pressure ratio 1:1. (a) TPR during first heating (0.5 K/s, 1×10^{-7} mbar NH_3), (b) TP-XPS during first heating (0.3 K/s, 5×10^{-8} mbar NH_3), (c) TPR during cooling (0.5 K/s, 1×10^{-7} mbar NH_3), and (c) TP-XPS during cooling (0.3 K/s, 5×10^{-8} mbar NH_3).

The observed reaction rate ($-\mathrm{d}[NH_3]/\mathrm{d}t \equiv \mathrm{d}[H_2O]/\mathrm{d}t$) decreased slightly with increasing temperature. It probably was limited by the availability of reactants at high temperature; that is, $NH_{3\,ad}$ desorption was competing with $NH_{3\,ad}$ dissociation [39].

In the cooling branch (Figs. 3c and d), N-selectivity changed back to N_2 at ∼900 K. The surface changed from O_{ad}- to N_{ad}-covered at about 600 K, and the surface oxygen concentration was close to zero below 500 K. The N_2 formation rate was low at 500 K, and the reaction stopped completely at 400 K, due to inhibition by $NH_{x\,ad}$, which blocks O_2 adsorption.

In the cooling branch no H_2 formation was observed, and the only reaction product containing hydrogen was water. This finding can be explained by hysteresis observed in the O_{ad} coverage. During the heating branch, the O_{ad} concentration was negligible at 400 K; it started to grow at 600 K, so not enough O_{ad} was available to react with all of the H_{ad} produced between 400 K and 600 K. In the cooling branch, O_{ad} was present down to 500 K, allowing H_2O formation at this temperature.

We also observed a slow decrease in the N_{ad} concentration in the cooling branch, even below 400 K. This decrease cannot be due to N_2 desorption, because N_2 desorption was not observed below 400 K in the cooling branch (see Fig. 3c). Therefore, we assigned the decrease in the N_{ad} coverage (Fig. 3d) to rehydrogenation of N_{ad} to NH_{ad} [39].

3.3. The influence of the NH_3:O_2 pressure ratio on the activity and selectivity

Fig. 4 shows the effect of the NH_3/O_2 pressure ratio on the observed reaction products and on the surface composition during reaction. The heating branch is shown for two different NH_3/O_2 ratios: 1:5 and 1:10.

An increase in O_2 partial pressure had little effect on the surface composition below 400 K. This finding is not surprising, because the surface was covered with O_{ad} and $NH_{x\,ad}$ and O_2 adsorption was inhibited by $NH_{x\,ad}$. Fig. 4 shows only the sum of $NH_{3\,ad}$ and NH_{ad}, not the individual traces, to simplify the figure. The greatest effect of the O_2 partial pressure was observed in the temperature range at which the surface changed from N_{ad}-covered to O_{ad}-covered. For a ratio of 1:5 (Figs. 4a and b), the change occurred at around 520 K (620 K for 1:1), whereas for a ratio of 1:10 (Fig. 4c and d), it occurred around 480 K. We did not observe H_2 formation for higher O_2 partial pressures, because O_{ad} in those cases was already available at 500 K, and H_2O could easily form.

A small influence of the oxygen partial pressure was observed in the gas phase below 400 K. The low-temperature N_2 desorption peak (300–500 K) was larger for higher O_2 partial pressure. At higher O_2 partial pressures, more O_2 reached the surface, the O_{ad} coverage was slightly higher and repulsive interactions are more pronounced. NO(g) formation shifted to lower temperature when the O_2 partial pressure was increased. For a ratio 1:5, NO(g) formation was observed above ∼800 K (900 K for 1:1), whereas for the ratio 1:10, NO(g) formation was observed above 600 K. For both ratios, NO was the only N-containing gas phase product above 850 K. We also observed NO_{ad} on the surface, which formed above 500 K (when the surface was O_{ad} covered) and was present on the surface up to 600 K, when it desorbed.

Fig. 5 shows the NO_{ad} concentrations for the ratios 1:5 and 1:10 (NO_{ad} was not observed for the ratio 1:1). In the heating branch NO_{ad} formed above 500 K. The NO_{ad} concentration started to decrease above 550 K. The NO_{ad} concentration slowly increased in the cooling branch between 600 and 450 K, reaching a constant value below 450 K. At these temperatures dissociation did not occur, and NO_{ad} was present on the surface as a spectator species.

The rate of H_2O formation (which is indicative of the overall reaction rate, $-\mathrm{d}[NH_3]/\mathrm{d}t \equiv \mathrm{d}[H_2O]/\mathrm{d}t$) is not influenced by the O_2 partial pressure. This means that the reaction is almost zeroth order in O_2 and oxygen adsorption and dissociation are not the rate-determining steps in the overall reaction.

A small desorption peak was observed for $m/e = 44$ around the temperature at which the surface composition changed to O_{ad}-covered and where N_{ad} and NO_{ad} coexisted on the surface. This could be due to N_2O, but the formation of CO_2 via reaction of O_{ad} and CO from the background cannot be excluded. Baerns et al. [2] recently published an extensive study on ammonia oxidation on Pt catalysts. They studied the reaction in different pressure regimes, ranging from 10^{-5} to 10^{3} mbar. They did not observe N_2O formation in the UHV experiments; they observed N_2O only for pressures higher than $\sim 1 \times 10^{-3}$ mbar. Their interpretation of their findings was that N_2O forms only when the concentration of both NO_{ad} and N_{ad} are sufficiently high. This is in line with our observations, because we saw N_2O formation only when both NO_{ad} and N_{ad} were present on the surface in measurable amounts. In our case the N_{ad} concentration dropped very fast above 500 K, with the N_{ad} availability possibly limiting N_2O formation.

3.4. NH_3 oxidation on Ir(111)

Fig. 6 shows the gas phase reaction products in the cooling branch of the $NH_3 + O_2$ reaction on Ir(111) for different reactant ratios. The first and second heating were very similar to the cooling branch, and hysteresis was not observed.

In the heating branch, the steady-state reaction started at ∼500 K (ratio 1:1); in the cooling branch, it stopped at the same temperature. This temperature decreased slightly when the O_2 partial pressure was increased. For an NH_3:O_2 ratio of 1:10, the steady-state reaction started at ∼400 K in the heating branch and stopped at the same temperature in the subsequent cooling branch. Below 500 K, the reaction products were N_2 and H_2O. For the ratio 1:1, some H_2 was observed around 500 K as well, but the main H-containing

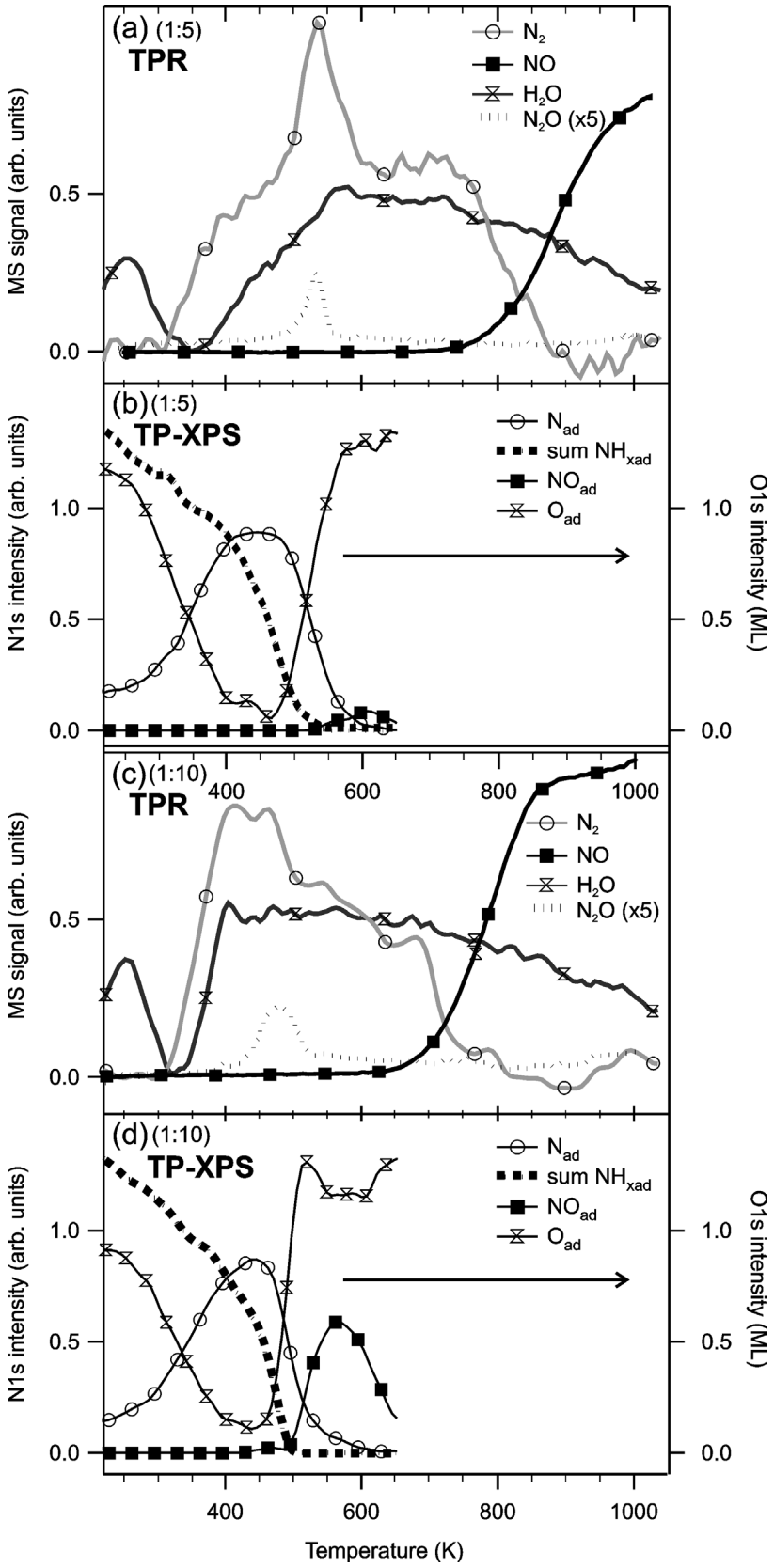

Fig. 4. The effect of the NH_3/O_2 ratio on the selectivity of the surface and on the nature of the reaction products (heating 1). (a) TPR (0.5 K/s, 1×10^{-7} mbar NH_3) and (b) TP-XPS (0.3 K/s, 5×10^{-8} mbar NH_3) for the NH_3/O_2 ratio 1:5; and (c) TPR (0.5 K/s, 1×10^{-7} mbar NH_3) and (d) TP-XPS (0.3 K/s, 5×10^{-8} mbar NH_3) for the ratio 1:10.

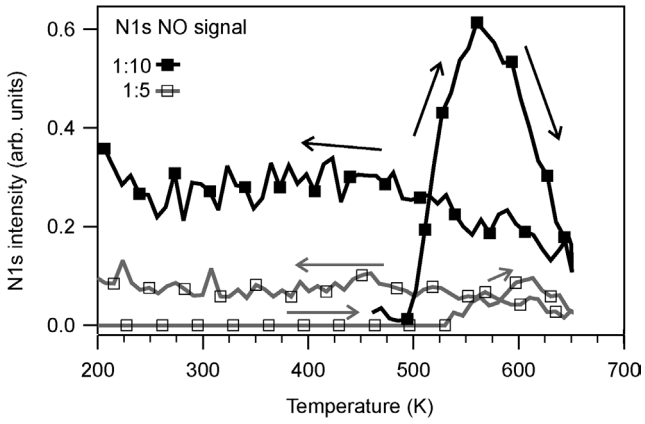

Fig. 5. TP-XPS data showing NO_{ad} (400.0 eV) formation during NH_3 oxidation for two different NH_3:O_2 pressure ratios (1:5 and 1:10, 0.3 K/s, 5×10^{-8} mbar NH_3).

product was always H_2O. NO was formed at higher temperatures, depending on the NH_3/O_2 ratio. For a ratio of 1:1, NO formed above 800 K, whereas for a ratio of 1:10, it formed above 500 K and for a ratio of 1:5 it formed above 600 K.

The results are similar to the results obtained for Ir(110). The temperature range where the reaction started and stopped was between 400 and 500 K for both surfaces. Moreover, a change in N-selectivity also occurred at similar temperatures.

A significant difference between Ir(111) and Ir(110) was that the reaction rate on Ir(111) increased much more with increasing O_2 partial pressure. On Ir(111), the reaction rate was almost first order in O_2 pressure, whereas on Ir(110), the reaction rate did not change significantly with increasing O_2 pressure. This indicates that O_2 adsorption and dissociation is a very important step on Ir(111), in contrast to what we found for Ir(110). This is in line with the results of TPD experiments presented in Section 3.1, which showed that chemisorbed oxygen is needed for $NH_{3\,ad}$ dissociation.

We assume that the mechanism responsible for the N-selectivity is similar on both Ir surfaces, because the selectivity of NH_3 oxidation on both surfaces showed similar behavior for different temperatures and different NH_3:O_2 pressure ratios. The mechanism responsible for NH_3 dissociation might be different because of the different reactivity of the surfaces. On Ir(111), we needed O_{ad} for the initial $NH_{3\,ad}$ dissociation step, whereas on Ir(110), it proceeded also in the absence of oxygen. On Ir(111), the reaction rate also strongly depended on the O_2 pressure and not on Ir(110).

3.5. The selectivity of the NH_3 oxidation on Ir(110) and Ir(111)

In Section 1 several issues were mentioned that are still under debate. One of these was the mechanism of N_2 and NO_{ad} formation. For both reactions, two possible mechanisms have been proposed, one involving only N_{ad} and O_{ad} and the other involving $NH_{x\,ad}$ and O_{ad}. In our previous study in the absence of O_{ad}, we showed [39] that N_2 forms via $N_{ad} + N_{ad}$ rather than via $NH_{x\,ad} + NH_{x\,ad}$. In the presence of O_{ad} on the surface, the NH_{ad} concentration is lower than in the absence of O_{ad} [40], and a mechanism involving $NH_{x\,ad}$ species is not likely. N_2 formation via a reaction between NO_{ad} and $NH_{3\,ad}$ is also not very likely, because NO_{ad} is observed only above 450 K, where the $NH_{3\,ad}$ concentration is very low.

In earlier work we showed [40] that NO_{ad} formation occurs via $N_{ad} + O_{ad}$ rather than via $NH_{x\,ad} + O_{ad}$, because the $NH_{x\,ad}$ concentration is negligible when the NO_{ad} formation starts. Fig. 4 shows the same thing: NO formation starts when the $NH_{x\,ad}$ concentration is zero.

The difference in selectivity between Pt and Ir catalysts is not yet completely understood. In the model proposed by Bradley, Hopkinson, and King (BHK) [8] for Pt(100) NO formation at low temperature and NO dissociation [3,29, 33] at higher temperature play a crucial role [Eqs. (5)–(9)]. NO_{ad} forms around 250 K on Pt(100) and dissociation starts at 350 K. TP-RAIRS experiments done by Kim, Pratt and King [26] show ed that NO_{ad} was present on Pt(100) between 250 and 500 K, in line with the BHK model.

In our measurements we monitored in situ all the surface species during the reaction (NO_{ad}, $NH_{3\,ad}$, NH_{ad}, N_{ad} and O_{ad}). Our results suggest that the BHK model cannot be applied to Ir(110) or Ir(111). In their model NO_{ad} is observed between 250 and 500 K, whereas in our measurements NO_{ad} formation is observed only above 500 K. NH_{ad}, N_{ad}, and O_{ad} coexist on the surface between 200 and 400 K and hence, in principle, NO_{ad} could be formed. This suggests that there is a kinetic limitation for the formation of NO_{ad}. The presence of NO_{ad} in the cooling branch, without dissociation, indicates that NO dissociation does not occur below 400 K. In our experiment the surface was always covered with O_{ad} when NO_{ad} was present. Because O_{ad} blocks NO dissociation [8,13,14] it is also very unlikely that NO dissociates in this temperature regime under reaction conditions.

During the reaction, Ir(110) surface composition changes at a certain temperature from $NH_{x\,ad}$ to O_{ad} (Fig. 4). The observed selectivity in the gas phase also changes from N_2 to NO, but the temperature at which this change takes place is 200 K higher than the observed change of surface composition. To explain this large difference, we need to look at some simple kinetic equations

$$\frac{\mathrm{d}[N_2]}{\mathrm{d}t} = k_{N_2}\theta_N^2, \tag{10}$$

$$\frac{\mathrm{d}[NO]}{\mathrm{d}t} = k_{NO}\theta_N\theta_O. \tag{11}$$

If k_{N_2} and k_{NO} would have the same value, then (i) the selectivity of the reaction (above the NO and N_2 desorption temperature, i.e., >600 K) would depend only on the N_{ad} and O_{ad} (θ_N and θ_O) coverage, and (ii) the selectivity change toward NO would occur at the same temperature as the change of the surface composition. Our results show that this is not the case, so differences in the k values instead of the coverages of the different species must be responsi-

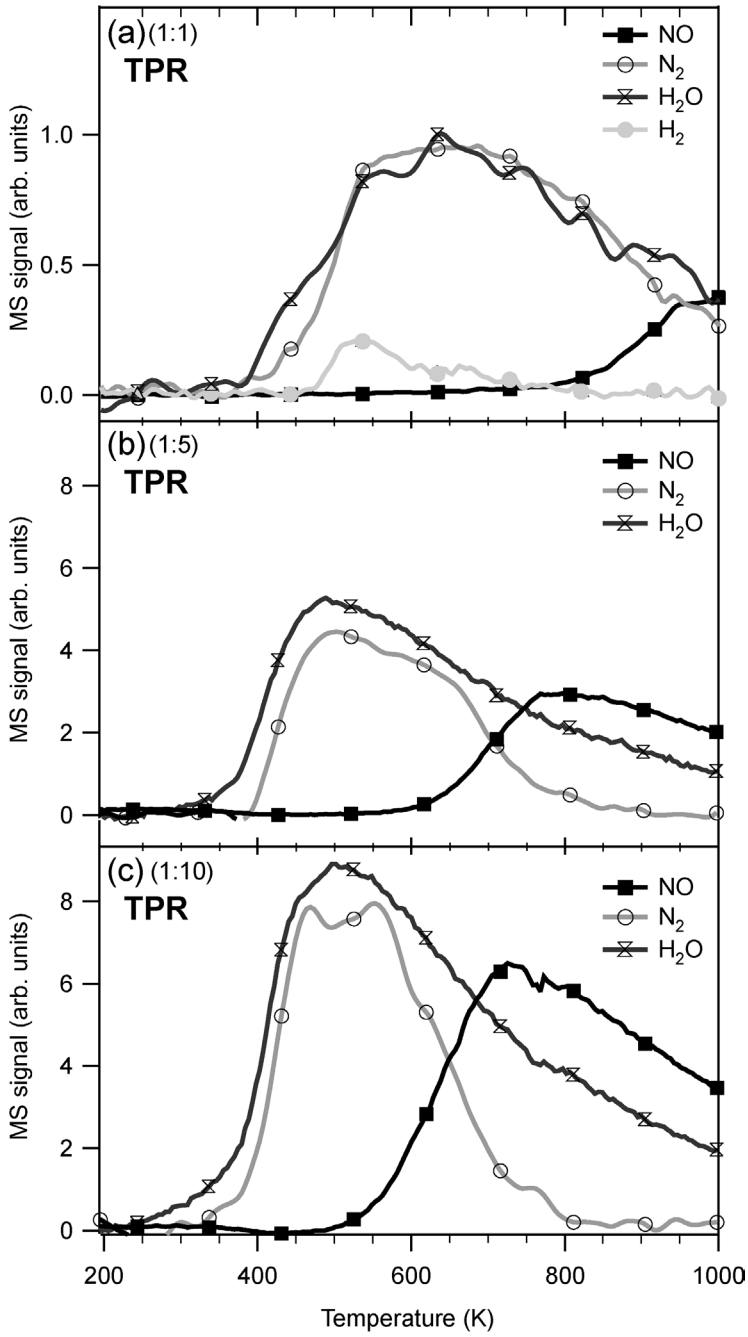

Fig. 6. TPR results for NH_3 oxidation on Ir(111). The cooling branch for different NH_3/O_2 pressure ratios (1:1, 1:5, 1:10) is shown (heating rate 0.5 K/s, 1×10^{-7} mbar NH_3).

ble for the observed difference between surface composition and product selectivity. The experimental results can be reproduced when we assume that k_{N_2} is larger than k_{NO}, that is, N_2 formation is easier than NO formation. The temperature dependence of the k values is described by the Arrhenius equation, $k = A_0 e^{-E_a/(RT)}$, where k is a prefactor and E_a is the activation energy. Because both N_2 and NO formation proceed via simple recombination reactions of N_{ad} + N_{ad} or N_{ad} + O_{ad} [39,40] the prefactors are expected to be rather similar for both NO_{ad} and N_2 formation [15]. In that case different k values should be related to differences in activation energies. This leads to the conclusion that the E_a is greater for NO formation than for N_2 formation.

Our recently published study concerning the effect of O_{ad} on the $NH_{3\,ad}$ chemistry on Ir(110) [40] gave more information on the activation energies for NO and N_2 formation. N_2 formation was observed around 600 K in TPD experiments. Heating of a mixed NH_3/O_{ad} layer in the presence of O_2(g) resulted in the formation of NO_{ad}, starting around 450 K. These two observations suggest that NO_{ad} forms more easily than N_2. We also found that N_2 formation is influenced

by the presence of O_2. In the presence of O_{ad}, N_2 formation occurs around 350 K, so in that case it is more easy than NO_{ad} formation.

In summary, we suggest that the difference between Pt and Ir surfaces during catalytic ammonia oxidation can be found in the lower activation energy for NO formation on Pt with respect to Ir. This contradicts earlier literature reports in which the difference was explained in terms of NO dissociation [38].

4. Summary and conclusions

We studied the adsorption and dissociation of NH_3 on Ir(111). Ammonia does not dissociate on this surface, but defects created by sputtering can facilitate $NH_{3\,ad}$ dissociation on this surface. O_{ad} also facilitates $NH_{3\,ad}$ dissociation and NH_3 adsorption on a sputtered surface and an oxygen-covered surface results in N_2 formation around 500 K.

We also studied the steady-state NH_3 oxidation reaction on Ir(110) and Ir(111) under low-pressure conditions. On both surfaces, the steady-state NH_3 oxidation reaction starts around 400 K (with the exact temperature depending on the NH_3/O_2 pressure ratio), the initial products being N_2 and H_2O. The surface composition changes around 500 K from $NH_{x\,ad}$ to O_{ad}, but the selectivity of the products observed in the gas phase changes at a significantly higher temperatures.

An increase in O_2 partial pressure greatly enhances the reaction rate on Ir(111)and enhances it by much less on Ir(110). This difference is explained by the fact that NH_3 dissociates on Ir(110) even in the absence of O_{ad}, whereas on Ir(111) O_{ad} is needed for significant NH_3 dissociation.

The different behavior of Ir and Pt catalysts during catalytic ammonia oxidation is explained in terms of the different activity of these metals in NO formation. NO_{ad} forms readily on Pt surfaces (above 300 K [26]), whereas on Ir, NO_{ad} formation occurs only above 450 K, in a large excess of O_{ad}. N_2 is more easily formed under these conditions (O_{ad} lowers the activation energy of N_2 formation) than is NO on Ir(110), resulting in preferential N_2(g) formation even when the surface is O_{ad}-covered.

Acknowledgments

The authors thank ELETTRA and the E.U. for financial support for the measurements at the SuperESCA beamline of ELETTRA. They also acknowledge R.C.V. van Schie for providing technical support. C.J.W. acknowledges the Technology Foundation STW, Applied Science Division of NWO and the Technology Program of the Ministry of Economic Affairs for financial support under project number UPC.5037. J.R.M. acknowledges the Socrates/Erasmus program for the opportunity to come to Leiden University. A.B. acknowledges financial support from the MIUR under program PRIN2003.

References

[1] B. Afsin, P.R. Davies, A. Paskusky, M.W. Roberts, D. Vincent, Surf. Sci. 284 (1993) 109–120.
[2] M. Baerns, R. Imbihl, V.A. Kondratenko, R. Kraehnert, W.K. Offermans, R.A. van Santen, A. Scheibe, J. Catal. 232 (2005) 226–238.
[3] W.F. Banholzer, R.I. Masel, Surf. Sci. 137 (1984) 339–360.
[4] A. Baraldi, M. Barnaba, B. Brena, D. Cocco, G. Comelli, S. Lizzit, G. Paolucci, R. Rosei, J. Electron. Spectrosc. Relat. Phenom. 76 (1995) 145–149.
[5] A. Baraldi, G. Comelli, S. Lizzit, D. Cocco, G. Paolucci, R. Rosei, Surf. Sci. 367 (3) (1995) L67–L72.
[6] A. Baraldi, G. Comelli, S. Lizzit, M. Kiskinova, G. Paolucci, Surf. Sci. Rep. 49 (6–8) (2003) 169–224.
[7] A. Baraldi, V.R. Dhanak, J. Electron Spectrosc. Relat. Phenom. 67 (1) (1994) 211–220.
[8] J.M. Bradley, A. Hopkinson, D.A. King, J. Phys. Chem. 99 (1995) 17032–17042.
[9] S.A.C. Carabineiro, B.E. Nieuwenhuys, Surf. Sci. 505 (2002) 163–170.
[10] S.A.C. Carabineiro, B.E. Nieuwenhuys, Surf. Sci. 532 (2003) 87–95.
[11] A.F. Carley, P.R. Davies, K.R. Harikumar, R.V. Jones, G.U. Kulkarni, M.W. Roberts, Top. Catal. 12 (1–4) (2001) 101–109.
[12] T.V. Choudhary, A.K. Santra, C. Sivadinaranaya, B.K. Min, C.-W. Yi, K. Davis, D.W. Goodman, Catal. Lett. 77 (1–3) (2001) 1–5.
[13] C.A. de Wolf, J.W. Bakker, P.T. Wouda, B.E. Nieuwenhuys, A. Baraldi, S. Lizzit, M. Kiskinova, J. Chem. Phys. 113 (2000) 10717–10722.
[14] C.A. de Wolf, J.W. Bakker, P.T. Wouda, B.E. Nieuwenhuys, A. Baraldi, S. Lizzit, M. Kiskinova, J. Phys. Chem. B. 105 (2001) 4254–4262.
[15] J.A. Dumesic, D.F. Rudd, L.M. Aparicio, J.E. Rekoske, A.A. Treviño, The Microkinetics of Heterogeneous Catalysis, American Chemical Society, 1993.
[16] A. Fahmi, R.A. van Santen, Z. Phys. Chem. 197 (1996) 203–217.
[17] H. Gerischer, A. Mauerer, J. Electroanal. Chem. 25 (1970) 421.
[18] J.M. Gohndrone, C.W. Olsen, A.L. Backman, T.R. Gow, E. Yagasaki, R.I. Masel, J. Vac. Sci. Technol. A 7 (3) (1988) 1986–1990.
[19] J.F. Gootzen, A.H. Wonders, W. Visscher, R.A. van Santen, J.A.R. van Veen, Electrochim. Acta 43 (1998) 1851.
[20] V.V. Gorodetskii, V.A. Sobyanin, in: T. Seiyama, K. Tanabe (Eds.), Proceedings of 7th International Congress on Catalysis, Elsevier and Kodansha LTD, Tokyo, 1980, pp. 566–577.
[21] H. Guo, D. Chrysostomou, J. Flowers, F. Zaera, J. Phys. Chem. B 107 (2003) 502–511.
[22] H. Guo, F. Zaera, Surf. Sci. 524 (2003) 1–14.
[23] W.L. Guthrie, J.D. Sokol, G.A. Somorjai, Surf. Sci. 109 (1981) 390–418.
[24] D.I. Hagen, B.E. Nieuwenhuys, G. Rovida, G.A. Somorjai, Surf. Sci. 57 (2) (1976) 632–650.
[25] J.J. Joyce, M. del Guidice, J.H. Weaver, J. Electron Spectrosc. Relat. Phenom. 49 (1) (1989) 31–45.
[26] M. Kim, S.J. Pratt, D.A. King, J. Am. Chem. Soc. 122 (2000) 2409–2410.
[27] W.P. Krekelberg, J. Greeley, M. Mavrikakis, J. Phys. Chem. B 108 (2004) 987–994.
[28] E.S. Kurkina, N.L. Semendyaeva, A.I. Boronin, Kinet. Catal. 42 (5) (2001) 773–789.
[29] R.I. Masel, Catal. Rev. Sci. Eng. 28 (1986) 335–369.
[30] W.D. Mieher, W. Ho, Surf. Sci. 322 (1995) 151.
[31] H. Mortensen, L. Diekhöner, A. Baurichter, E. Jensen, A.C. Luntz, J. Chem. Phys. 113 (16) (2000) 6882–6887.
[32] R.J. Purtell, P. Merrill, Phys. Rev. Lett. 44 (19) (1980) 1279–1281.
[33] E.D.L. Rienks, J.W. Bakker, A. Baraldi, S.A.C. Carabineiro, S. Lizzit, C.J. Weststrate, B.E. Nieuwenhuys, Surf. Sci. 516 (2002) 109–117.

[34] A.K. Santra, B.K. Min, C.W. Yi, K. Luo, T.V. Choudhary, D.W. Goodman, J. Phys. Chem. B 106 (2001) 340–344.
[35] D.P. Sobczyk, A.M. de Jong, E.J.M. Hensen, R.A. van Santen, J. Catal. 219 (2003) 156–166.
[36] J.L. Taylor, D.E. Ibbotson, W.H. Weinberg, Surf. Sci. 79 (2) (1979) 349–384.
[37] D.M. Thornburg, R.J. Madix, Surf. Sci. 220 (2–3) (1989) 268–294.
[38] A.C.M. van den Broek, J. van Grondelle, R.A. van Santen, J. Catal. 185 (1999) 297–306.
[39] C.J. Weststrate, J.W. Bakker, E.D.L. Rienks, S. Lizzit, L. Petaccia, A. Baraldi, C.P. Vinod, B.E. Nieuwenhuys, J. Chem. Phys. 122 (18) (2005) 184705.
[40] C.J. Weststrate, J.W. Bakker, E.D.L. Rienks, S. Lizzit, L. Petaccia, A. Baraldi, C.P. Vinod, B.E. Nieuwenhuys, Phys. Chem. Chem. Phys. 7 (13) (2005) 2629–2634.